

# Semileptonic $D_q \rightarrow K_1 \ell \nu$ and nonleptonic $D \rightarrow K_1 \pi$ decays in three-point QCD sum rules and factorization approach

R. Khosravi<sup>1 \*</sup>, K. Azizi<sup>2 †</sup>, N. Ghahramany<sup>1 ‡</sup>

<sup>1</sup> Physics Department, Shiraz University, Shiraz 71454, Iran

<sup>2</sup> Department of Physics, Middle East Technical University, 06531 Ankara, Turkey

## Abstract

We analyze the semileptonic  $D_q \rightarrow K_1 \ell \nu$  transition with  $q = u, d, s$ , in the framework of the three-point QCD sum rules and the nonleptonic  $D \rightarrow K_1 \pi$  decay within the QCD factorization approach. We study  $D_q$  to  $K_1(1270)$  and  $K_1(1400)$  transition form factors by separating the mixture of the  $K_1(1270)$  and  $K_1(1400)$  states. Using the transition form factors of the  $D \rightarrow K_1$ , we analyze the nonleptonic  $D \rightarrow K_1 \pi$  decay. We also present the decay amplitude and decay width of these decays in terms of the transition form factors. The branching ratios of these channel modes are also calculated at different values of the mixing angle  $\theta_{K_1}$  and compared with the existing experimental data for the nonleptonic case.

PACS: 11.55.Hx, 13.20.Fc, 12.39.St

---

\*e-mail: khosravi.reza @ gmail.com

†e-mail: e146342 @ metu.edu.tr

‡e-mail: ghahramany @ susc.ac.ir

# 1 Introduction

Analyzing the semileptonic decays of the charmed  $D_q$  mesons is very useful for determination of the elements of the Cabibbo-Kabayashi-Maskawa (CKM) matrix and also leptonic decay constants of the initial and final meson states. The semileptonic  $D_s \rightarrow K_1 \ell \nu$  transition could give useful information about the internal structure of the  $D_s$  meson. Investigating the nonleptonic decays such as  $D \rightarrow K_1 \pi$  can also be important for interpretation of the structure of the lightest scalar mesons [1].

From the experimental view, the physical states  $K_1(1270)$  and  $K_1(1400)$  are the mixtures of the strange members of two axial-vector  $SU(3)$  octets  $1^3P_1(K_{1A})$  and  $1^1P_1(K_{1B})$ . The  $K_{1A}$  and  $K_{1B}$  are not mass eigenstates and they can be mixed together due to the nonstrange light quark mass difference. Their relations with the  $K_1(1270)$  and  $K_1(1400)$  states can be written as [2–4]:

$$\begin{aligned} |K_1(1270)\rangle &= |K_{1A}\rangle \sin\theta_{K_1} + |K_{1B}\rangle \cos\theta_{K_1}, \\ |K_1(1400)\rangle &= |K_{1A}\rangle \cos\theta_{K_1} - |K_{1B}\rangle \sin\theta_{K_1}. \end{aligned} \quad (1)$$

The angle  $\theta_{K_1}$  has been obtained with two-fold ambiguity  $|\theta_{K_1}| \approx 33^\circ$ , as given in Ref [3]. Also in Ref [6]  $35^\circ \leq |\theta_{K_1}| \leq 55^\circ$  has been found. In this paper we use  $\theta_{K_1}$  in the interval  $37^\circ \leq |\theta_{K_1}| \leq 58^\circ$  [4, 7]. The sign ambiguity for  $\theta_{K_1}$  is due to the fact that one can add arbitrary phases to  $|K_{1A}\rangle$  and  $|K_{1B}\rangle$  states.

The QCD sum rules approach has been successfully applied to a wide variety of problems in charm meson decays. The semileptonic decays  $D_s \rightarrow f_0 \ell \nu$ ,  $D_s \rightarrow \phi \ell \nu$  [1],  $D \rightarrow \bar{K}^0 \ell \nu$  [8],  $D^+ \rightarrow K^{0*} e^+ \nu_e$  [9],  $D \rightarrow \pi \ell \nu$  [10],  $D \rightarrow \rho \ell \nu$  [11],  $D_s^+ \rightarrow \phi \ell \nu$  [12] and  $D \rightarrow K_0^* \bar{\ell} \nu$  [13] have been studied in the framework of the three-point QCD sum rules. As a nonperturbative method, the QCD sum rules has been of interest and it is a well established technique in the hadron physics since it is based on the fundamental QCD Lagrangian (for details about the QCD sum rules approach see for instance [14]).

In the present work, we study the semileptonic decays of the  $D_q \rightarrow K_1 \ell \nu$  in the framework of the three-point QCD sum rules. The long distance dynamics of such transitions can be parameterized in terms of some form factors calculating of which play fundamental role in the analyzing of such type transitions. Considering the contributions of the operators with mass dimension  $d = 3, 4, 5$  as condensate and non-perturbative contributions, first we calculate the transition form factors of the semileptonic  $D_q \rightarrow K_1 \ell \nu$  ( $q = u, d, s$ ) decays. Using these form factors, the total decay width as well as the branching ratio for the aforementioned transitions are also evaluated at different values of the mixing angle. Having computed the form factors of the  $D \rightarrow K_1$ , the amplitude and decay rate of the nonleptonic  $D_{u,d} \rightarrow K_1 \pi$  decays are also computed in terms of those form factors using the QCD factorization method (for more about the method see [15–17] and references therein).

The paper is organized as follows. The calculation of the sum rules for the relevant form factors are presented in section2. In calculating the form factors, first we consider the general  $\langle K_1 |$  state. Then, using the definition of the G-parity conserving decay constant  $\langle 0 | J_{K_{1A}}^\nu | K_{1A}(p', \varepsilon) \rangle = f_{K_{1A}} m_{K_{1A}} \varepsilon^\nu$  and G-parity violating decay constant  $\langle 0 | J_{K_{1B}}^\nu | K_{1B}(p', \varepsilon) \rangle = f_{K_{1B^\perp}} (1 \text{ GeV}) a_0^{\parallel, K_{1B}} m_{K_{1B}} \varepsilon^\nu$ , where  $a_0^{\parallel, K_{1B}}$  is the zeroth Gegenbauer moment

of  $K_{1B}$  state and it is zero in the  $SU(3)$  symmetry limit, we obtain the form factors of the  $D \rightarrow K_{1A(B)}$  states. Finally, considering Eq. (1), we separate the  $\langle K_1[1270(1400)] \rangle$  states and derive form factors of the  $D \rightarrow K_1[1270(1400)]$  transitions. The decay rate formulas for semileptonic and nonleptonic cases are presented in section 3. We derive the decay rate formula for  $D \rightarrow K_1\pi$  decay using the QCD factorization method in tree level. Section 4 is devoted to the numeric analysis of the form factors as well as the branching fractions of the considered semileptonic and non-leptonic decays at different values of the mixing angle, and discussions. A comparison of our results for the branching ratios for the non-leptonic case with the existing experimental data is also made in this section.

## 2 Sum rules for $D_q \rightarrow K_1\ell\nu$ transition form factors

The  $D_q \rightarrow K_1\ell\nu$  with  $q = u, d, s$  decay governed by the tree level  $c \rightarrow q'$  ( $q' = d, s$ ) transition (see Fig. 1).

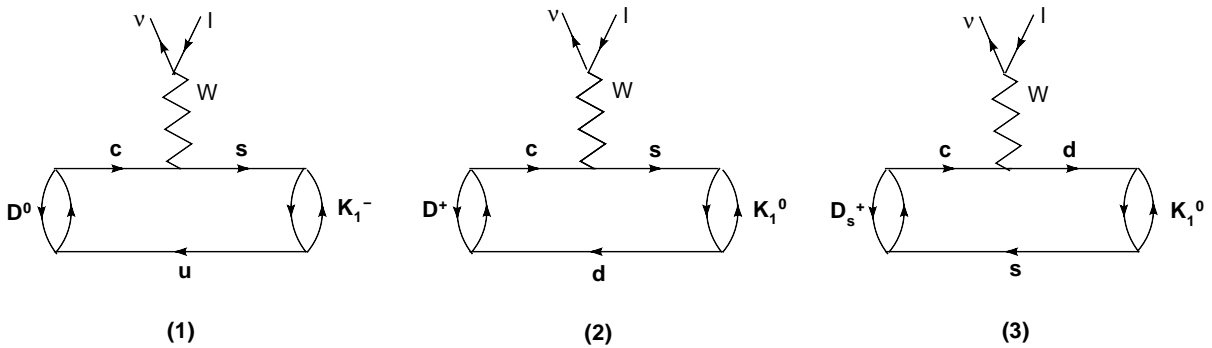


Figure 1: Semileptonic decays of  $D_q$  to  $K_1$ . Diagrams 1, 2 and 3 are related to the  $D^0 \rightarrow K_1^-\ell\nu$ ,  $D^+ \rightarrow K_1^0\ell\nu$  and  $D_s^+ \rightarrow K_1^0\ell\nu$ , respectively.

In the standard model, the effective Hamiltonian responsible for these transitions is given as:

$$\mathcal{H}_{eff} = \frac{G_F}{\sqrt{2}} V_{cq'} \bar{\nu} \gamma_\mu (1 - \gamma_5) l \bar{q}' \gamma_\mu (1 - \gamma_5) c, \quad (2)$$

where,  $G_F$  is the Fermi constant and  $V_{cq'}$  are the CKM matrix elements. The decay amplitude for  $D_q \rightarrow K_1\ell\nu$  is obtained by inserting Eq. (2) between the initial and final meson states.

$$\mathcal{M} = \frac{G_F}{\sqrt{2}} V_{cq'} \bar{\nu} \gamma_\mu (1 - \gamma_5) l \langle K_1(p', \varepsilon) | \bar{q}' \gamma_\mu (1 - \gamma_5) c | D_q(p) \rangle. \quad (3)$$

The next step is to calculate the matrix element appearing in Eq. (3). Both axial and vector parts of the transition current give contribution to this matrix element and it can be parametrized in terms of some form factors using the Lorentz invariance and parity conservation as follows:

$$\langle K_1(p', \varepsilon) | \bar{q}' \gamma_\mu \gamma_5 c | D_q(p) \rangle = -\frac{2f_V^{D_q \rightarrow K_1}(q^2)}{(m_{D_q} + m_{K_1})} \epsilon_{\mu\nu\alpha\beta} \varepsilon^\nu p^\alpha p'^\beta, \quad (4)$$

$$\begin{aligned} \langle K_1(p', \varepsilon) | \bar{q}' \gamma_\mu c | D_q(p) \rangle &= i \left[ f_0^{D_q \rightarrow K_1}(q^2)(m_{D_q} + m_{K_1})\varepsilon_\mu \right. \\ &\quad \left. - \frac{f_1^{D_q \rightarrow K_1}(q^2)}{(m_{D_q} + m_{K_1})}(\varepsilon p)P_\mu - \frac{f_2^{D_q \rightarrow K_1}(q^2)}{(m_{D_q} + m_{K_1})}(\varepsilon p)q_\mu \right]. \end{aligned} \quad (5)$$

In order for the calculations to be simple, the following redefinitions are used

$$\begin{aligned} F_V^{D(s) \rightarrow K_1}(q^2) &= \frac{2f_V^{D_q \rightarrow K_1}(q^2)}{(m_{D_q} + m_{K_1})}, & F_0^{D_q \rightarrow K_1}(q^2) &= f_0^{D_q \rightarrow K_1}(q^2)(m_{D_q} + m_{K_1}), \\ F_1^{D_q \rightarrow K_1}(q^2) &= -\frac{f_1^{D_q \rightarrow K_1}(q^2)}{(m_{D_q} + m_{K_1})}, & F_2^{D_q \rightarrow K_1}(q^2) &= -\frac{f_2^{D_q \rightarrow K_1}(q^2)}{(m_{D_q} + m_{K_1})}, \end{aligned} \quad (6)$$

where the  $F_V^{D_q \rightarrow K_1}(q^2)$ ,  $F_0^{D_q \rightarrow K_1}(q^2)$ ,  $F_1^{D_q \rightarrow K_1}(q^2)$  and  $F_2^{D_q \rightarrow K_1}(q^2)$  are the new transition form factors,  $P_\mu = (p + p')_\mu$ ,  $q_\mu = (p - p')_\mu$  and  $\varepsilon$  is the four-polarization vector of the axial  $K_1$  meson.

Based on the general philosophy of the three-point QCD sum rules technique, the above form factors in Eq. (6) can be evaluated from the time ordered product of the following three currents.

$$\Pi_{\mu\nu}^{(V-A)}(p^2, p'^2, q^2) = i^2 \int d^4x d^4y e^{+ip'x - ipy} \langle 0 | T \{ J_{K_1\nu}(x) J_\mu^{(V-A)}(0) J_{D_q}^\dagger(y) \} | 0 \rangle, \quad (7)$$

where,  $J_{K_1\nu}(x) = \bar{q}_1 \gamma_\nu \gamma_5 s$  ( $q_1 = u, d$ ),  $J_{D_q}(y) = \bar{q} \gamma_5 c$  are the interpolating currents of the  $K_1^{0-}$  and  $D_q$  and  $J_\mu^V = \bar{q}' \gamma_\mu c$  and  $J_\mu^A = \bar{q}' \gamma_\mu \gamma_5 c$  are the vector and axial-vector parts of the transition current, respectively.

The above correlation function is calculated in two different approaches: On the quark level, it describes a meson as quarks and gluons interacting in a QCD vacuum. This is called the theoretical or QCD side. In the phenomenological or physical side, it is saturated by a tower of mesons with the same quantum numbers as the interpolating currents. The form factors are determined by matching these two different representations of the correlation function and applying double Borel transformation with respect to the momentum of the initial and final meson states to suppress the contribution coming from the higher states and continuum. We can express the correlation function in both sides in terms of four independent Lorentz structures:

$$\Pi_{\mu\nu}^{(V-A)} = \epsilon_{\mu\nu\alpha\beta} p^\alpha p'^\beta \Pi_V + g_{\mu\nu} \Pi_0 + P_\mu p_\nu \Pi_1 + q_\mu p_\nu \Pi_2. \quad (8)$$

To find the sum rules for the related form factors, we will match the coefficients of the corresponding structures from both representations of the correlation function.

First, we calculate the aforementioned correlation function in the phenomenological representation. Inserting two complete sets of intermediate states with the same quantum number as the currents  $J_{K_1}$  and  $J_{D_q}$  to Eq. (7), we obtain

$$\begin{aligned} \Pi_{\mu\nu}^{V-A}(p^2, p'^2, q^2) &= \\ &= \frac{\langle 0 | J_{K_1\nu} | K_1(p', \varepsilon) \rangle \langle K_1(p', \varepsilon) | J_\mu^{V-A} | D_q(p) \rangle \langle D_q(p) | J_{D_q}^\dagger | 0 \rangle}{(p'^2 - m_{K_1}^2)(p^2 - m_{D_q}^2)} + \\ &\quad \text{the higher resonances and continuum.} \end{aligned} \quad (9)$$

In Eq. (9), the vacuum to initial and final meson states matrix elements are defined as:

$$\langle 0 | J_{K_1}^\nu | K_1(p') \rangle = f_{K_1} m_{K_1} \varepsilon^\nu, \quad \langle 0 | J_{D_q} | D_q(p) \rangle = i \frac{f_{D_q} m_{D_q}^2}{m_c + m_q}, \quad (10)$$

where  $f_{K_1}$  and  $f_{D_q}$  are the leptonic decay constants of  $K_1$  and  $D_q$  mesons, respectively. Using Eq. (4), Eq. (5) and Eq. (10) in Eq. (9) and performing summation over the polarization vector of the  $K_1$  meson, we get the following result for the physical part:

$$\begin{aligned} \Pi_{\mu\nu}^{V-A}(p^2, p'^2, q^2) &= -\frac{f_{D_q} m_{D_q}^2}{(m_c + m_q)} \frac{f_{K_1} m_{K_1}}{(p'^2 - m_{K_1}^2)(p^2 - m_{D_q}^2)} \times [F_0^{D(s) \rightarrow K_1}(q^2) g_{\mu\nu} \\ &+ F_1^{D(s) \rightarrow K_1}(q^2) P_\mu p_\nu + F_2^{D(s) \rightarrow K_1}(q^2) q_\mu p_\nu + i F_V^{D(s) \rightarrow K_1}(q^2) \epsilon_{\mu\nu\alpha\beta} p'^\alpha p^\beta] \\ &+ \text{excited states.} \end{aligned} \quad (11)$$

The coefficients of the Lorentz structures  $i\epsilon_{\mu\nu\alpha\beta} p^\alpha p'^\beta$ ,  $g_{\mu\nu}$ ,  $P_\mu p_\nu$  and  $q_\mu p_\nu$  in the correlation function  $\Pi_{\mu\nu}^{V-A}$  will be chosen in determination of the form factors  $F_V^{D(s) \rightarrow K_1}(q^2)$ ,  $F_0^{D(s) \rightarrow K_1}(q^2)$ ,  $F_1^{D(s) \rightarrow K_1}(q^2)$  and  $F_2^{D(s) \rightarrow K_1}(q^2)$ , respectively.

On the QCD or theoretical side, the correlation function is calculated in the quark and gluon languages by the help of the operator product expansion (OPE) in the deep Euclidean region where  $p^2 \ll (m_c + m_q)^2$ ,  $p'^2 \ll (m_q^2 + m_q'^2)$ . In Eq. (7), using the expansion of the time ordered products of the currents, the three-point correlation function is written in terms of the series of local operators with increasing dimension as the following form [18]:

$$\begin{aligned} -\int d^4x d^4y e^{i(px-p'y)} T \{ J_{K_1\nu} J_\mu J_{D_q}^\dagger \} &= (C_0)_{\mu\nu} I + (C_3)_{\mu\nu} \bar{\Psi} \Psi + (C_4)_{\mu\nu} G_{\alpha\beta} G^{\alpha\beta} \\ &+ (C_5)_{\mu\nu} \bar{\Psi} \sigma_{\alpha\beta} G^{\alpha\beta} \Psi + (C_6)_{\mu\nu} \bar{\Psi} \Gamma \Psi \bar{\Psi} \Gamma' \Psi, \end{aligned} \quad (12)$$

where,  $G_{\alpha\beta}$  is the gluon field strength tensor,  $(C_i)_{\mu\nu}$  are the Wilson coefficients,  $I$  is the unit matrix,  $\Psi$  is the local field operator of the light quarks, and  $\Gamma$  and  $\Gamma'$  are the matrices appearing in the calculations. Taking into account the vacuum expectation value of the OPE, the expansion of the correlation function in terms of the local operators is written as follows:

$$\begin{aligned} \Pi_{\mu\nu}(p_1^2, p_2^2, q^2) &= C_{0\mu\nu} + C_{3\mu\nu} \langle \bar{\Psi} \Psi \rangle + C_{4\mu\nu} \langle G^2 \rangle + C_{5\mu\nu} \langle \bar{\Psi} \sigma_{\alpha\beta} G^{\alpha\beta} \Psi \rangle \\ &+ C_{6\mu\nu} \langle \bar{\Psi} \Gamma \Psi \bar{\Psi} \Gamma' \Psi \rangle. \end{aligned} \quad (13)$$

In Eq.(13), the contributions of the perturbative and condensate terms of dimension 3, 4, and 5 as non-perturbative parts are considered. The diagrams for the contributions of the non-perturbative part are depicted in Figs. 2, 3 and 4. It's found that the heavy quark condensate contributions are suppressed by inverse of the heavy quark mass and can be safely removed (see diagrams 4, 5, 6 in Fig. 2). The light  $q'$  quark condensate contributions are zero after applying the double Borel transformation with respect to both variables  $p^2$  and  $p'^2$  since only one variable appears in the denominator (see diagrams 1, 2, 3 in Fig. 2).

Our calculations show that in this case, the two-gluon condensate contributions (see diagrams in Fig. 3) are very small in comparison with the quark condensate contributions

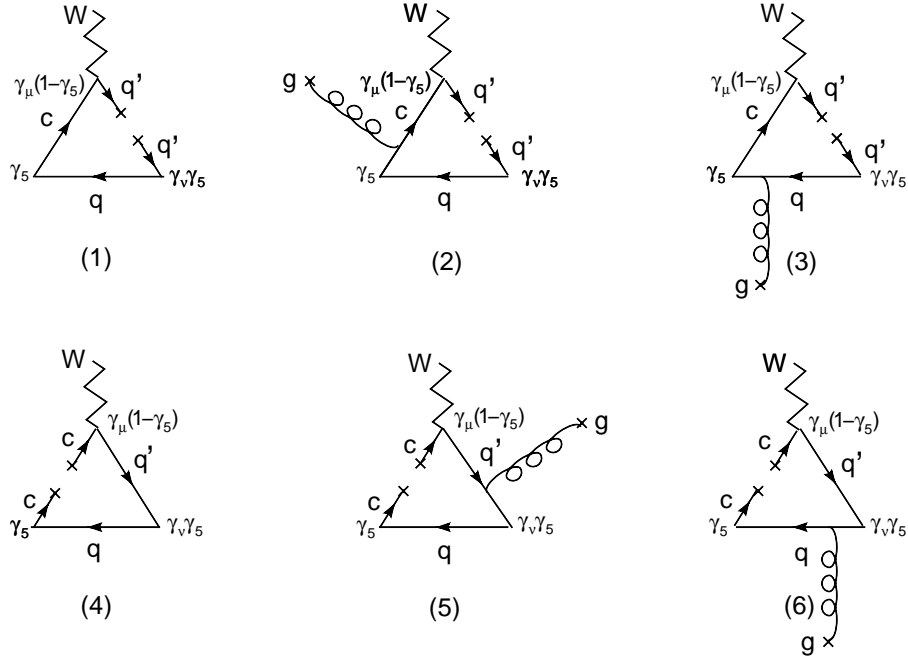


Figure 2: The quark condensate diagrams without any gluon and with one gluon emission.

and we can easily ignore their contributions in our calculations.

Therefore, the main contribution in the non-perturbative part comes from the q-quark condensates. (see Fig. 4).

As a result, in the lowest order of the perturbation theory, the three-point correlation function receives a contribution from the perturbative part (bare-loop contributions of diagrams in Fig. 1) and non-perturbative part (contributions of the diagrams shown in Fig. 4) i.e.,

$$\Pi_i(p^2, p'^2, q^2) = \Pi_i^{per}(p^2, p'^2, q^2) + \Pi_i^{non-per}(p^2, p'^2, q^2). \quad (14)$$

Using the double dispersion representation, the bare-loop contribution is determined:

$$\Pi_i^{per} = -\frac{1}{(2\pi)^2} \int \int \frac{\rho_i^{per}(s, s', q^2)}{(s-p^2)(s'-p'^2)} ds ds' + \text{subtraction terms}, \quad (15)$$

The following inequality is responsible for obtaining the integration limits in Eq. (15).

$$-1 \leq \frac{2ss' + (s + s' - q^2)(m_c^2 - m_q^2 - s) + 2s(m_q^2 - m_{q'}^2)}{\lambda^{1/2}(s, s', q^2)\lambda^{1/2}(m_c^2, m_q^2, s)} \leq +1, \quad (16)$$

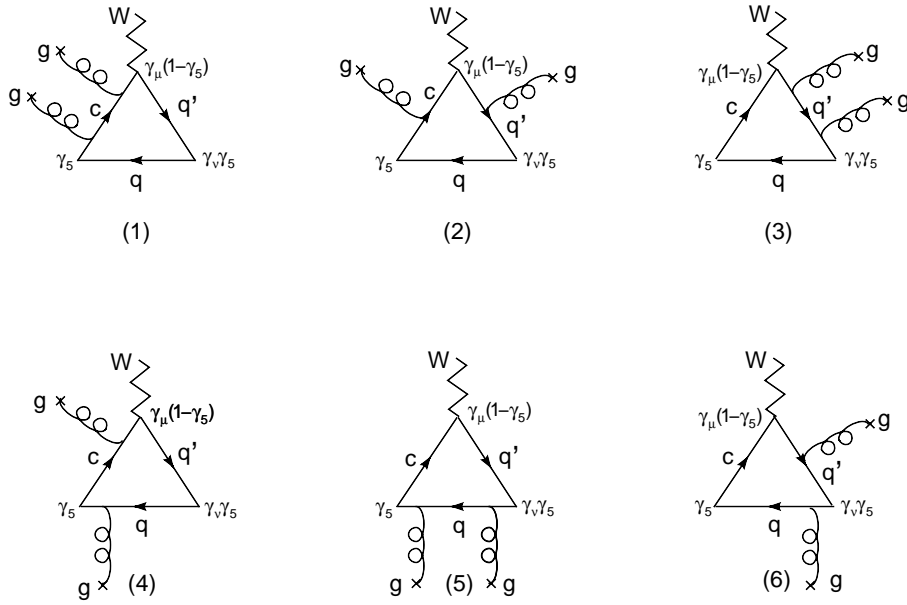


Figure 3: Diagrams for two-gluon condensate contributions.

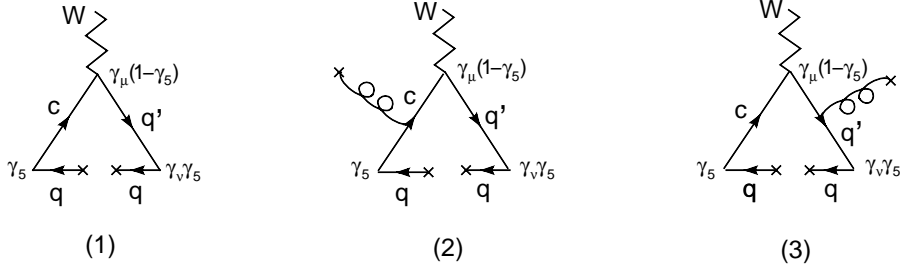


Figure 4: Diagrams for q-quark condensates contributions.

where  $\lambda(a, b, c) = a^2 + b^2 + c^2 - 2ab - 2ac - 2bc$  is the usual triangle function.

By the help of the Cutkosky rule, i.e., replacing the propagators with the Dirac-delta functions:

$$\frac{1}{k^2 - m^2} \rightarrow -2i\pi\delta(k^2 - m^2), \quad (17)$$

the spectral densities  $\rho_i^{per}(s, s', q^2)$  are found as:

$$\rho_V = 4N_c I_0(s, s', q^2) \{B_1(m_c - m_q) - B_2(m_{q'} + m_q) - m_q\},$$

$$\rho_0 = -2N_c I_0(s, s', q^2) \{\Delta(m_q + m_{q'}) - \Delta'(m_c - m_q) - 4A_1(m_c - m_q) + 2m_q^2(m_c - m_q - m_{q'}) + m_q(2m_c m_{q'} - u)\},$$

$$\rho_1 = 2N_c I_0(s, s', q^2) \{B_1(m_c - 3m_q) - B_2(m_q + m_{q'}) + 2A_2(m_c - m_q) + 2A_3(m_c - m_q) - m_q\},$$

$$\begin{aligned} \rho_2 = & 2N_c I_0(s, s', q^2) \{ 2A_2(m_c - m_q) - 2A_3(m_c - m_q) - B_1(m_c + m_q) \\ & + B_2(m_q + m_{q'}) + m_q \} . \end{aligned} \tag{18}$$

where

$$\begin{aligned} I_0(s, s', q^2) &= \frac{1}{4\lambda^{1/2}(s, s', q^2)}, \\ \lambda(s, s', q^2) &= s^2 + s'^2 + q^4 - 2sq^2 - 2s'q^2 - 2ss', \\ B_1 &= \frac{1}{\lambda(s, s', q^2)} [2s'\Delta - \Delta'u], \\ B_2 &= \frac{1}{\lambda(s, s', q^2)} [2s\Delta' - \Delta u], \\ A_1 &= \frac{1}{2\lambda(s, s', q^2)} [\Delta'^2 s + \Delta^2 s' - 4m_q^2 ss' - \Delta\Delta'u + m_q^2 u^2], \\ A_2 &= \frac{1}{\lambda^2(s, s', q^2)} [2\Delta'^2 ss' + 6\Delta^2 s'^2 - 8m_q^2 ss'^2 - 6\Delta\Delta' s'u \\ &\quad + \Delta'^2 u^2 + 2m_q^2 s'u^2], \\ A_3 &= \frac{1}{\lambda^2(s, s', q^2)} [-3\Delta^2 us' - 3\Delta'^2 us + 4m_q^2 us's + 4\Delta\Delta' ss' \\ &\quad + 2\Delta\Delta' u^2 - m_q^2 u^3], \end{aligned}$$

where,  $u = s + s' - q^2$ ,  $\Delta = s + m_q^2 - m_c^2$ ,  $\Delta' = s' + m_q^2 - m_{q'}^2$  and  $N_c = 3$  is the color factor.

The corresponding non-perturbative part of the considered structures are obtained as follows:

$$\begin{aligned} \Pi_V^{non-per}(p^2, p'^2, q^2) = & \langle q\bar{q} \rangle \left\{ \frac{1}{2} \frac{m_q m_{q'}}{r r'^2} - \frac{1}{2} \frac{m_q m_c}{r^2 r'} - \frac{m_{q'}^2 m_q^2}{r r'^3} + \frac{1}{2} \frac{m_{q'}^2 m_0^2}{r r'^3} \right. \\ & - \frac{1}{2} \frac{m_c^2 m_q^2}{r^2 r'^2} + \frac{1}{3} \frac{m_0^2 m_c^2}{r^2 r'^2} - \frac{1}{2} \frac{m_{q'}^2 m_q^2}{r^2 r'^2} + \frac{1}{3} \frac{m_{q'}^2 m_0^2}{r^2 r'^2} + \frac{1}{2} \frac{q^2 m_q^2}{r^2 r'^2} \\ & \left. - \frac{1}{3} \frac{m_0^2 q^2}{r^2 r'^2} - \frac{m_c^2 m_q^2}{r^3 r'} + \frac{1}{2} \frac{m_0^2 m_c^2}{r^3 r'} + \frac{1}{6} \frac{m_0^2 m_c m_{q'}}{r^2 r'^2} + \frac{1}{3} \frac{m_0^2}{r^2 r'} \right\}, \end{aligned} \tag{19}$$

$$\begin{aligned} \Pi_0^{non-per}(p^2, p'^2, q^2) = & \langle q\bar{q} \rangle \left\{ -\frac{1}{4} \frac{m_q m_{q'}}{r r'} - \frac{1}{4} \frac{m_q m_c^3}{r^2 r'} - \frac{1}{4} \frac{m_q m_c}{r r'} + \frac{1}{4} \frac{m_0^2 m_c^2}{r^2 r'} \right. \\ & \left. + \frac{1}{4} \frac{m_0^2 m_{q'}^2}{r^2 r'} - \frac{1}{3} \frac{m_0^2 q^2}{r^2 r'} + \frac{1}{6} \frac{m_0^2 m_c^4}{r^2 r'^2} + \frac{1}{6} \frac{m_0^2 m_{q'}^4}{r^2 r'^2} + \frac{1}{6} \frac{m_0^2 q^4}{r^2 r'^2} \right\} \end{aligned}$$



$$\begin{aligned}
& + \frac{1}{6} \frac{m_0^2 m_c^2}{r r'^2} + \frac{1}{4} \frac{m_0^2 m_{q'}^2}{r r'^2} - \frac{1}{6} \frac{m_0^2 q^2}{r r'^2} + \frac{1}{4} \frac{m_q m_{q'}^3}{r r'^2} - \frac{1}{2} \frac{m_{q'}^4 m_q^2}{r r'^3} \\
& + \frac{1}{4} \frac{m_0^2 m_{q'}^4}{r r'^3} - \frac{1}{4} \frac{m_c^4 m_q^2}{r^2 r'^2} - \frac{1}{4} \frac{m_c^2 m_q^2}{r^2 r'} - \frac{1}{4} \frac{m_{q'}^2 m_q^2}{r^2 r'} + \frac{1}{4} \frac{q^2 m_q^2}{r^2 r'} \\
& - \frac{1}{4} \frac{m_{q'}^4 m_q^2}{r^2 r'^2} - \frac{1}{4} \frac{m_{q'}^2 m_q^2}{r r'^2} - \frac{1}{6} \frac{m_0^2}{r r'} - \frac{3}{4} \frac{m_0^2 m_c m_{q'}}{r^2 r'} + \frac{1}{6} \frac{m_0^2 m_c^2 m_{q'}^2}{r^2 r'^2} \\
& - \frac{1}{3} \frac{m_0^2 m_c^2 q^2}{r^2 r'^2} - \frac{1}{3} \frac{m_0^2 m_{q'}^2 q^2}{r^2 r'^2} + \frac{1}{2} \frac{m_q m_c^2 m_{q'}}{r^2 r'} - \frac{1}{4} \frac{m_q m_c m_{q'}^2}{r^2 r'} \\
& + \frac{1}{4} \frac{m_q m_c q^2}{r^2 r'} - \frac{1}{4} \frac{m_q m_{q'} q^2}{r r'^2} + \frac{1}{4} \frac{m_q m_c^2 m_{q'}}{r r'^2} - \frac{1}{2} \frac{m_q m_c m_{q'}^2}{r r'^2} + \frac{1}{2} \frac{m_q^2}{r r'} \\
& - \frac{1}{4} \frac{m_c^2 m_q^2}{r r'^2} - \frac{1}{4} \frac{q^4 m_q^2}{r^2 r'^2} + \frac{1}{4} \frac{q^2 m_q^2}{r r'^2} - \frac{1}{2} \frac{m_c^4 m_q^2}{r^3 r'} + \frac{1}{4} \frac{m_c^4 m_0^2}{r^3 r'} \\
& + \frac{1}{2} \frac{m_c m_{q'} m_q^2}{r^2 r'} + \frac{1}{2} \frac{m_c m_{q'} m_q^2}{r r'^2} - \frac{1}{4} \frac{m_c m_{q'} m_0^2}{r r'^2} + \frac{m_c^3 m_{q'} m_q^2}{r^3 r'} \\
& - \frac{1}{2} \frac{m_c^3 m_{q'} m_0^2}{r^3 r'} - \frac{1}{2} \frac{m_c^2 m_{q'}^2 m_q^2}{r^3 r'} + \frac{1}{4} \frac{m_c^2 m_{q'}^2 m_0^2}{r^3 r'} + \frac{1}{2} \frac{m_c^2 q^2 m_q^2}{r^3 r'} \\
& - \frac{1}{4} \frac{m_0^2 m_c^2 q^2}{r^3 r'} + \frac{1}{2} \frac{m_c^2 q^2 m_q^2}{r^2 r'^2} - \frac{1}{2} \frac{m_c m_{q'} q^2 m_q^2}{r^2 r'^2} + \frac{1}{4} \frac{m_c m_{q'} q^2 m_0^2}{r^2 r'^2} \\
& + \frac{1}{2} \frac{m_{q'}^2 q^2 m_q^2}{r^2 r'^2} - \frac{1}{2} \frac{m_c^2 m_{q'}^2 m_q^2}{r r'^3} + \frac{1}{4} \frac{m_c^2 m_{q'}^2 m_0^2}{r r'^3} + \frac{m_c m_{q'}^3 m_q^2}{r r'^3} \\
& - \frac{1}{2} \frac{m_c m_{q'}^3 m_0^2}{r r'^3} + \frac{1}{2} \frac{m_{q'}^2 q^2 m_q^2}{r r'^3} - \frac{1}{4} \frac{m_0^2 m_{q'}^2 q^2}{r r'^3} + \frac{1}{2} \frac{m_c^3 m_{q'} m_q^2}{r^2 r'^2} \\
& - \frac{1}{4} \frac{m_c^3 m_{q'} m_0^2}{r^2 r'^2} - \frac{1}{2} \frac{m_c^2 m_{q'}^2 m_q^2}{r^2 r'^2} + \frac{1}{2} \frac{m_c m_{q'}^3 m_q^2}{r^2 r'^2} - \frac{1}{4} \frac{m_c m_{q'}^3 m_0^2}{r^2 r'^2} \Big\} , \tag{20}
\end{aligned}$$

$$\begin{aligned}
\Pi_1^{non-per}(p^2, p'^2, q^2) &= \langle q\bar{q} \rangle \left\{ -\frac{1}{4} \frac{m_q m_{q'}}{r r'^2} + \frac{1}{4} \frac{m_q m_c}{r^2 r'} + \frac{1}{2} \frac{m_{q'}^2 m_q^2}{r r'^3} - \frac{1}{4} \frac{m_{q'}^2 m_0^2}{r r'^3} \right. \\
& + \frac{1}{4} \frac{m_c^2 m_q^2}{r^2 r'^2} - \frac{1}{6} \frac{m_0^2 m_c^2}{r^2 r'^2} + \frac{1}{4} \frac{m_{q'}^2 m_q^2}{r^2 r'^2} - \frac{1}{6} \frac{m_{q'}^2 m_0^2}{r^2 r'^2} - \frac{1}{4} \frac{q^2 m_q^2}{r^2 r'^2} \\
& + \frac{1}{6} \frac{m_0^2 q^2}{r^2 r'^2} + \frac{1}{2} \frac{m_c^2 m_q^2}{r^3 r'} - \frac{1}{4} \frac{m_0^2 m_c^2}{r^3 r'} - \frac{1}{2} \frac{m_q^2}{r^2 r'} + \frac{1}{6} \frac{m_0^2}{r^2 r'} \\
& \left. - \frac{1}{12} \frac{m_0^2 m_c m_{q'}}{r^2 r'^2} \right\} , \tag{21}
\end{aligned}$$

$$\begin{aligned}
\Pi_2^{non-per}(p^2, p'^2, q^2) &= \langle q\bar{q} \rangle \left\{ \frac{1}{4} \frac{m_q m_{q'}}{r r'^2} - \frac{1}{4} \frac{m_q m_c}{r^2 r'} - \frac{1}{2} \frac{m_{q'}^2 m_q^2}{r r'^3} + \frac{1}{4} \frac{m_{q'}^2 m_0^2}{r r'^3} \right. \\
& - \frac{1}{4} \frac{m_c^2 m_q^2}{r^2 r'^2} + \frac{1}{6} \frac{m_0^2 m_c^2}{r^2 r'^2} - \frac{1}{4} \frac{m_{q'}^2 m_q^2}{r^2 r'^2} + \frac{1}{6} \frac{m_{q'}^2 m_0^2}{r^2 r'^2} + \frac{1}{4} \frac{q^2 m_q^2}{r^2 r'^2} \\
& - \frac{1}{6} \frac{m_0^2 q^2}{r^2 r'^2} - \frac{1}{2} \frac{m_c^2 m_q^2}{r^3 r'} + \frac{1}{4} \frac{m_0^2 m_c^2}{r^3 r'} - \frac{1}{2} \frac{m_q^2}{r^2 r'} + \frac{1}{2} \frac{m_0^2}{r^2 r'} \\
& \left. + \frac{1}{12} \frac{m_0^2 m_c m_{q'}}{r^2 r'^2} \right\} . \tag{22}
\end{aligned}$$

where  $r = p^2 - m_c^2$ ,  $r' = p'^2 - m_{q'}^2$ .

Equating two representations of the correlation function and applying the double Borel transformation using

$$\begin{aligned}\mathcal{B}_{p^2}(M_1^2)\left(\frac{1}{p^2 - m_c^2}\right)^m &= \frac{(-1)^m}{\Gamma(m)} \frac{e^{-\frac{m_c^2}{M_1^2}}}{(M_1^2)^m}, \\ \mathcal{B}_{p'^2}(M_2^2)\left(\frac{1}{p'^2 - m_{q'}^2}\right)^n &= \frac{(-1)^n}{\Gamma(n)} \frac{e^{-\frac{m_{q'}^2}{M_2^2}}}{(M_2^2)^n},\end{aligned}\quad (23)$$

the sum rules for the form factors  $F_i^{D(s) \rightarrow K_1}$  are obtained as:

$$\begin{aligned}F_i^{D(s) \rightarrow K_1} &= -\frac{(m_c + m_q)}{f_{D_q} m_{D_q}^2 f_{K_1} m_{K_1}} e^{\frac{m_{D_q}^2}{M_1^2}} e^{\frac{m_{K_1}^2}{M_2^2}} \left\{ -\frac{1}{4\pi^2} \int_{m_c^2}^{s'_0} ds' \int_{s_L}^{s_0} ds \rho_i(s, s', q^2) e^{\frac{-s}{M_1^2}} e^{\frac{-s'}{M_2^2}} \right. \\ &\quad \left. + M_1^2 M_2^2 \mathcal{B}_{p^2}(M_1^2) \mathcal{B}_{p'^2}(M_2^2) [\Pi_i^{non-per}(p^2, p'^2, q^2)] \right\},\end{aligned}\quad (24)$$

where  $i = V, 0, 1$  and  $2$ ,  $s_0$  and  $s'_0$  are the continuum thresholds in pseudoscalar  $D_q$  and axial-vector  $K_1$  channels, respectively and the lower limit in the integration over  $s$  is as follows:

$$s_L = \frac{(m_q^2 + q^2 - m_c^2 - s')(m_c^2 s' - m_q^2 q^2)}{(m_c^2 - q^2)(m_q^2 - s')}. \quad (25)$$

In Eq. (24), to subtract the contributions of the higher states and the continuum the quark-hadron duality assumption is also used, i.e., it is assumed that

$$\rho^{higherstates}(s, s') = \rho^{OPE}(s, s') \theta(s - s_0) \theta(s - s'_0). \quad (26)$$

Here, we should stress that in the three-point sum rules with double dispersion relation, the subtraction of the continuum states and the quark-hadron duality is highly nontrivial. For  $q^2 > 0$  values, there may be an inconsistency between double dispersion integrals in Eq. (24) and corresponding coefficients of the structures in the Feynman amplitudes in the bare-loop diagram. In this case, the double spectral density receives contributions beyond the contributions coming from the Landau-type singularities. This problem has been widely discussed in [9]. Here, we neglect such contributions since with the above continuum subtraction and the selecting integration region the contribution of the non-Landau singularities is very small comparing the Landau type singularity contributions.

Now, as we mentioned in the introduction section, the  $F_i^{D_q \rightarrow K_{1A(B)}}$  form factors are obtained from the above equation by replacing  $f_{K_1}$  by the G-parity conserving decay constant  $f_{K_{1A}}$  and G-parity violating decay constant  $f_{K_{1B}} = f_{K_{1B\perp}} (1 \text{ GeV}) a_0^{\parallel, K_{1B}}$  and  $m_{K_1}$  with  $m_{K_{1A(B)}}$ , i.e.,

$$\begin{aligned}F_i^{D(s) \rightarrow K_{1A(B)}} &= -\frac{(m_c + m_q)}{f_{D_q} m_{D_q}^2 f_{K_{1A(B)}} m_{K_{1A(B)}}} e^{\frac{m_{D_q}^2}{M_1^2}} e^{\frac{m_{K_{1A(B)}}^2}{M_2^2}} \left\{ -\frac{1}{4\pi^2} \int_{m_c^2}^{s'_0} ds' \int_{s_L}^{s_0} ds \rho_i(s, s', q^2) e^{\frac{-s}{M_1^2}} e^{\frac{-s'}{M_2^2}} \right. \\ &\quad \left. + M_1^2 M_2^2 \mathcal{B}_{p^2}(M_1^2) \mathcal{B}_{p'^2}(M_2^2) [\Pi_i^{non-per}(p^2, p'^2, q^2)] \right\}.\end{aligned}\quad (27)$$

Also, using Eqs. (1, 4, 5, 6), the form factors of the  $f_i^{D_q \rightarrow K_1[1270(1400)]}$  are found as follows:

$$\begin{aligned}
f_0^{D_q \rightarrow K_1(1270)} &= \left( \frac{m_{D_q} + m_{K_{1A}}}{m_{D_q} + m_{K_1}} \right) f_0^{D_q \rightarrow K_{1A}} \sin\theta_{K_1} + \left( \frac{m_{D_q} + m_{K_{1B}}}{m_{D_q} + m_{K_1}} \right) f_0^{D_q \rightarrow K_{1B}} \cos\theta_{K_1} , \\
f_{1,2,V}^{D_q \rightarrow K_1(1270)} &= \left( \frac{m_{D_q} + m_{K_1}}{m_{D_q} + m_{K_{1A}}} \right) f_{1,2,V}^{D_q \rightarrow K_{1A}} \sin\theta_{K_1} + \left( \frac{m_{D_q} + m_{K_1}}{m_{D_q} + m_{K_{1B}}} \right) f_{1,2,V}^{D_q \rightarrow K_{1B}} \cos\theta_{K_1} , \\
f_0^{D_q \rightarrow K_1(1400)} &= \left( \frac{m_{D_q} + m_{K_{1A}}}{m_{D_q} + m_{K_1}} \right) f_0^{D_q \rightarrow K_{1A}} \cos\theta_{K_1} - \left( \frac{m_{D_q} + m_{K_{1B}}}{m_{D_q} + m_{K_1}} \right) f_0^{D_q \rightarrow K_{1B}} \sin\theta_{K_1} , \\
f_{1,2,V}^{D_q \rightarrow K_1(1400)} &= \left( \frac{m_{D_q} + m_{K_1}}{m_{D_q} + m_{K_{1A}}} \right) f_{1,2,V}^{D_q \rightarrow K_{1A}} \cos\theta_{K_1} - \left( \frac{m_{D_q} + m_{K_1}}{m_{D_q} + m_{K_{1B}}} \right) f_{1,2,V}^{D_q \rightarrow K_{1B}} \sin\theta_{K_1} .
\end{aligned} \tag{28}$$

### 3 Decay amplitudes and decay widths

#### semileptonic

Using the amplitude in Eq. (3) and definitions of the form factors, the differential decay widths for the process  $D_q \rightarrow K_1 \ell \nu$  are found as follows:

$$\begin{aligned}
\frac{d\Gamma_{\pm}(D_q \rightarrow K_1 \ell \nu)}{dq^2} &= \frac{G_F^2 |V_{cq'}|^2}{192\pi^3 m_{D_q}^3} q^2 \lambda^{1/2}(m_{D_q}^2, m_{K_1}^2, q^2) |H_{\pm}|^2 , \\
\frac{d\Gamma_0(D_q \rightarrow K_1 \ell \nu)}{dq^2} &= \frac{G_F^2 |V_{cq'}|^2}{192\pi^3 m_{D_q}^3} q^2 \lambda^{1/2}(m_{D_q}^2, m_{K_1}^2, q^2) |H_0|^2 ,
\end{aligned} \tag{29}$$

where,

$$\begin{aligned}
H_{\pm}(q^2) &= (m_{D_q} + m_{K_1}) f_0(q^2) \mp \frac{\lambda^{1/2}(m_{D_q}^2, m_{K_1}^2, q^2)}{m_{D_q} + m_{K_1}} f_V(q^2) , \\
H_0(q^2) &= \frac{1}{2m_{K_1} \sqrt{q^2}} \left[ (m_{D_q}^2 - m_{K_1}^2 - q^2)(m_{D_q} + m_{K_1}) f_0(q^2) - \frac{\lambda(m_{D_q}^2, m_{K_1}^2, q^2)}{m_{D_q} + m_{K_1}} f_1(q^2) \right] .
\end{aligned}$$

The  $\pm, 0$  in the above relations belong to the  $K_1$  helicities. The total differential decay width can be written as

$$\frac{d\Gamma_{tot}(D_q \rightarrow K_1 \ell \nu)}{dq^2} = \frac{d\Gamma_L(D_q \rightarrow K_1 \ell \nu)}{dq^2} + \frac{d\Gamma_T(D_q \rightarrow K_1 \ell \nu)}{dq^2} , \tag{30}$$

where,

$$\begin{aligned}
\frac{d\Gamma_L(D_q \rightarrow K_1 \ell \nu)}{dq^2} &= \frac{d\Gamma_0(D_q \rightarrow K_1 \ell \nu)}{dq^2} , \\
\frac{d\Gamma_T(D_q \rightarrow K_1 \ell \nu)}{dq^2} &= \frac{d\Gamma_+(D_q \rightarrow K_1 \ell \nu)}{dq^2} + \frac{d\Gamma_-(D_q \rightarrow K_1 \ell \nu)}{dq^2} ,
\end{aligned} \tag{31}$$

and  $\frac{d\Gamma_L}{dq^2}$  ( $\frac{d\Gamma_T}{dq^2}$ ) is the longitudinal (transverse) component of the differential decay width.

## nonleptonic

In this part, we study the decay amplitude and decay width for the nonleptonic  $D \rightarrow K_1\pi$  decay. The effective Hamiltonian for this decay at the quark level is given by (see for example [19] and references therein):

$$H_{eff} = \frac{G_F}{\sqrt{2}} \{V_{cs}V_{ud}^*(C_1O_1 + C_2O_2)\}. \quad (32)$$

Here  $O_1$  and  $O_2$  are quark operators and they are given as:

$$O_1 = (\bar{s}_i c_i)_{V-A} (\bar{u}_j d_j)_{V-A}, \quad O_2 = (\bar{s}_i c_j)_{V-A} (\bar{u}_j d_i)_{V-A}, \quad (33)$$

where  $(\bar{q}_1 q_2)_{V\pm A} = \bar{q}_1 \gamma^\mu (1 \pm \gamma_5) q_2$ .

The Wilson coefficients  $C_1$  and  $C_2$  have been calculated in different schemes [20]. In the present work, we will use  $C_1(m_c) = 1.263$  and  $C_2(m_c) = -0.513$  obtained at the leading order in renormalization group improved perturbation theory at  $\mu \simeq 1.3 \text{ GeV}$  [21].

Now, we calculate the amplitude  $\mathcal{A}$  for  $D \rightarrow K_1\pi$  decay. Using the factorization method and definition of the related matrix elements in terms of the form factors  $f_V^{D \rightarrow K_1}$ ,  $f_0^{D \rightarrow K_1}$ ,  $f_1^{D \rightarrow K_1}$  and  $f_2^{D \rightarrow K_1}$  in Eqs. (4-6), we obtain this amplitude as follows:

$$\mathcal{A}^{D \rightarrow K_1\pi} = \frac{G_F}{\sqrt{2}} \{V_{cs}V_{ud}^* a_1\} f_\pi(\varepsilon \cdot p) [F^{D \rightarrow K_1\pi}(m_\pi^2)], \quad (34)$$

where,

$$F^{D \rightarrow K_1\pi}(m_\pi^2) = [(m_D + m_{K_1})f_0(m_\pi^2) - (m_D - m_{K_1})f_1(m_\pi^2) - \frac{f_2(m_\pi^2)}{(m_D + m_{K_1})}m_\pi^2]. \quad (35)$$

The  $\varepsilon$  stands for polarization of  $K_1$ ,  $p$  is four momentum of  $D$ ,  $f_\pi$  is the pion decay constant,  $a_1 = C_1 + \frac{1}{N_c}C_2$  and  $N_c$  is the number of colors in QCD.

Now, we can calculate the decay width for  $D \rightarrow K_1\pi$  decay. The explicit expression for decay width is given as follow:

$$\Gamma(D \rightarrow K_1\pi) = \frac{G_F^2}{128 \pi m_D^3 m_{K_1}^2} |V_{cs}|^2 |V_{ud}|^2 a_1^2 f_\pi^2 \lambda(m_D^2, m_{K_1}^2, m_\pi^2)^{\frac{3}{2}} [F^{D \rightarrow K_1\pi}(m_\pi^2)]^2. \quad (36)$$

## 4 Numerical analysis

From the sum rules expressions of the form factors, it is clear that the main input parameters entering the expressions are condensates, elements of the CKM matrix  $V_{cq'}$ , leptonic decay constants  $f_{D_q}$ ,  $f_{K_1A}$  and  $f_{K_{1B\perp}}$ , Borel parameters  $M_1^2$  and  $M_2^2$  as well as the continuum thresholds  $s_0$  and  $s'_0$ . We choose the values of the condensates (at a fixed renormalization scale of about  $1 \text{ GeV}$ ), leptonic decay constants, CKM matrix elements, quark and meson masses as:  $\langle u\bar{u} \rangle = \langle d\bar{d} \rangle = -(0.240 \pm 0.010 \text{ GeV})^3$ ,  $\langle s\bar{s} \rangle = (0.8 \pm 0.2) \langle u\bar{u} \rangle$ ,  $m_0^2 = 0.8 \pm 0.2 \text{ GeV}^2$  [22],  $|V_{cs}| = 0.957 \pm 0.110$ ,  $|V_{cd}| = 0.230 \pm 0.011$  [23],  $f_{D^0} =$

$f_{D^\pm} = 0.222 \pm 0.016 \text{ GeV}$  [24],  $f_{D_s} = 0.274 \pm 0.013 \text{ GeV}$  [25],  $f_{K_{1A}} = 0.250 \pm 0.013 \text{ GeV}$ ,  $f_{K_{1B^\perp}} = 0.190 \pm 0.010 \text{ GeV}$  [2],  $m_u(1 \text{ GeV}) = (1.5-3.3) \text{ MeV}$ ,  $m_d(1 \text{ GeV}) = (3.5-6) \text{ MeV}$ ,  $m_s(1 \text{ GeV}) = (104_{-34}^{+26}) \text{ MeV}$ ,  $m_c = 1.27_{-0.11}^{+0.07} \text{ GeV}$ ,  $m_{D^0} = 1.864 \text{ GeV}$ ,  $m_{D^\pm} = 1.869 \text{ GeV}$ ,  $m_{D_s} = 1.968 \text{ GeV}$ ,  $m_{K_1(1270)} = 1.27 \text{ GeV}$ ,  $m_{K_1(1400)} = 1.40 \text{ GeV}$  [23],  $m_{K_{1A}} = 1.31 \pm 0.06 \text{ GeV}$ ,  $m_{K_{1B}} = 1.34 \pm 0.08 \text{ GeV}$  and  $a_0^{\parallel, K_{1B}} = -0.19 \pm 0.07$  [2].

The sum rules for the form factors contain also four auxiliary parameters: Borel mass squares  $M_1^2$  and  $M_2^2$  and continuum thresholds  $s_0$  and  $s'_0$ . These are not physical quantities, so the form factors as physical quantities should be independent of them. The parameters  $s_0$  and  $s'_0$ , which are the continuum thresholds of  $D_q$  and  $K_1$  mesons, respectively, are determined from the condition that guarantees the sum rules to practically be stable in the allowed regions for  $M_1^2$  and  $M_2^2$ . The values of the continuum thresholds calculated from the two-point QCD sum rules are taken to be  $s_0 = (6-8) \text{ GeV}^2$  and  $s'_0 = (4-6) \text{ GeV}^2$ . The working regions for  $M_1^2$  and  $M_2^2$  are determined requiring that not only the contributions of the higher states and continuum are small, but the contributions of the operators with higher dimensions are also small. Both conditions are satisfied in the regions  $4 \text{ GeV}^2 \leq M_1^2 \leq 10 \text{ GeV}^2$  and  $3 \text{ GeV}^2 \leq M_2^2 \leq 8 \text{ GeV}^2$ .

The values of the form factors at  $q^2 = 0$  are shown in Tables 1 and 2. Note that, the values of the  $f_i(0)$  for  $D^0 \rightarrow K_1^\pm \ell \nu$  and  $D^\pm \rightarrow K_1^0 \ell \nu$  are approximately equal, so the values in Table. 1 refer to both decays.

$\theta_{K_1}^\circ$	37	58	-37	-58	$\theta_{K_1}^\circ$	37	58	-37	-58
$f_V^{D \rightarrow K_1(1270)}$	3.19	1.82	4.00	2.95	$f_V^{D \rightarrow K_1(1400)}$	-3.37	-4.34	2.27	3.60
$f_0^{D \rightarrow K_1(1270)}$	-0.74	-0.42	-0.93	-0.68	$f_0^{D \rightarrow K_1(1400)}$	0.72	0.92	-0.49	-0.77
$f_1^{D \rightarrow K_1(1270)}$	0.34	0.19	0.44	0.34	$f_1^{D \rightarrow K_1(1400)}$	-0.38	-0.49	0.23	0.38
$f_2^{D \rightarrow K_1(1270)}$	2.56	1.46	3.24	2.36	$f_2^{D \rightarrow K_1(1400)}$	-2.70	-3.49	1.82	2.90

Table 1: The  $q^2 = 0$  values of the form factors of the  $D \rightarrow K_1 \ell \nu$  decay for  $M_1^2 = 8 \text{ GeV}^2$ ,  $M_2^2 = 6 \text{ GeV}^2$  at different values of  $\theta_{K_1}$ .

The dependence of the  $f_i^{D_q \rightarrow K_1}(0)$  on  $\theta_{K_1}$  at  $q^2 = 0$  is depicted in Figs. 5-8, in the interval  $-58^\circ \leq \theta_{K_1} \leq 58^\circ$ . In Figs. 6 and 8, as it is seen, all of the form factors contact at one point. Also each form factor in Figs. 5 and 7, has one extremum point. These extrema as well as the contact points have been specified in Figs. 5-8. It is interesting that in the  $D_q \rightarrow K_1(1270) \ell \nu$  and  $D_q \rightarrow K_1(1400) \ell \nu$  cases, the extrema and contact points of the form factors are nearly at  $-8^\circ$ . The sum rules for the form factors are truncated at about  $q^2 = 0.15 \text{ GeV}^2$  and  $q^2 = 0.25 \text{ GeV}^2$  for  $q = u(d)$  and s cases of the  $K_1(1270)$ , respectively. These points for  $K_1(1400)$  state are  $q^2 = 0.22 \text{ GeV}^2$  and  $q^2 = 0.32 \text{ GeV}^2$  for u(d) and s cases, respectively. To extend the results to the full physical region, i.e.,  $0 \leq q^2 \leq (m_{D_q} - m_{K_1})^2 \text{ GeV}^2$ , we look for a parametrization such that: 1) this parametrization coincides well with the sum rules predictions below the points at which the form factors are truncated and 2) the parametrization provides an extrapolation to  $q^2 >$  the

$\theta_{K_1}^\circ$	37	58	-37	-58	$\theta_{K_1}^\circ$	37	58	-37	-58
$f_V^{D_s^+ \rightarrow K_1^0(1270)}$	3.90	2.22	4.86	3.58	$f_V^{D_s^+ \rightarrow K_1^0(1400)}$	-4.09	-5.27	2.76	4.40
$f_0^{D_s^+ \rightarrow K_1^0(1270)}$	-1.15	-0.65	-1.44	-1.07	$f_0^{D_s^+ \rightarrow K_1^0(1400)}$	1.12	1.44	-0.76	-1.20
$f_1^{D_s^+ \rightarrow K_1^0(1270)}$	-0.54	-0.31	-0.66	-0.50	$f_1^{D_s^+ \rightarrow K_1^0(1400)}$	0.57	0.73	-0.39	-0.61
$f_2^{D_s^+ \rightarrow K_1^0(1270)}$	5.89	3.36	7.33	5.40	$f_2^{D_s^+ \rightarrow K_1^0(1400)}$	-6.19	-7.97	4.18	6.64

Table 2: The  $q^2 = 0$  values of the form factors of the  $D_s \rightarrow K_1 \ell \nu$  decay for  $M_1^2 = 8 \text{ GeV}^2$ ,  $M_2^2 = 6 \text{ GeV}^2$  at different values of  $\theta_{K_1}$ .

truncated points, which is consistent with the expected analytical properties of the form factors and reproduces the lowest-lying resonance (pole). This resonance in the  $D_q$  channel is  $D^*(J^P = 1^-)$  state. Following references [26, 27], which describe this point in details, we choose the following theoretically more reliable fit parametrization:

$$f_i(q^2) = \frac{a}{1 - \frac{q^2}{m_{D^*}^2}} + \frac{b}{1 - \frac{q^2}{m_{fit}^2}}. \quad (37)$$

The values of the parameters  $a$ ,  $b$  and  $m_{fit}$  are given in Tables 3-6 at different values of the mixing angle  $\theta_{K_1}$ . From this parametrization, we see that the  $m_{D^*}$  pole exist outside the allowed physical region and related to that, one can calculate the hadronic parameters such as the coupling constant  $g_{DD^*K_1}$  (see [28, 29]).

	$a$	$b$	$m_{fit}$		$a$	$b$	$m_{fit}$
$f_V^{D \rightarrow K_1(1270)}(q^2)$	3.83	-0.64	1.25	$f_V^{D \rightarrow K_1(1400)}(q^2)$	-5.94	2.57	1.25
$f_0^{D \rightarrow K_1(1270)}(q^2)$	-2.05	1.31	1.36	$f_0^{D \rightarrow K_1(1400)}(q^2)$	2.04	-1.32	1.36
$f_1^{D \rightarrow K_1(1270)}(q^2)$	0.46	-0.12	1.27	$f_1^{D \rightarrow K_1(1400)}(q^2)$	-0.59	0.21	1.27
$f_2^{D \rightarrow K_1(1270)}(q^2)$	2.97	-0.41	1.29	$f_2^{D \rightarrow K_1(1400)}(q^2)$	-3.14	0.44	1.29
$f_V^{D_s^+ \rightarrow K_1^0(1270)}(q^2)$	4.08	-0.18	1.28	$f_V^{D_s^+ \rightarrow K_1^0(1400)}(q^2)$	-7.87	3.78	1.28
$f_0^{D_s^+ \rightarrow K_1^0(1270)}(q^2)$	-3.56	2.41	1.51	$f_0^{D_s^+ \rightarrow K_1^0(1400)}(q^2)$	3.06	-1.94	1.51
$f_1^{D_s^+ \rightarrow K_1^0(1270)}(q^2)$	-0.70	0.16	1.31	$f_1^{D_s^+ \rightarrow K_1^0(1400)}(q^2)$	0.58	-0.01	1.31
$f_2^{D_s^+ \rightarrow K_1^0(1270)}(q^2)$	7.12	-1.23	1.35	$f_2^{D_s^+ \rightarrow K_1^0(1400)}(q^2)$	-5.32	-0.87	1.35

Table 3: Parameters appearing in the fit function for the form factors of the  $D_q \rightarrow K_1(1270)\ell\nu$  and  $D_q \rightarrow K_1(1400)\ell\nu$  decays at  $M_1^2 = 8 \text{ GeV}^2$ ,  $M_2^2 = 6 \text{ GeV}^2$  and  $\theta_{K_1} = 37^\circ$ .

	$a$	$b$	$m_{fit}$		$a$	$b$	$m_{fit}$
$f_V^{D \rightarrow K_1(1270)}(q^2)$	2.12	-0.30	1.27	$f_V^{D \rightarrow K_1(1400)}(q^2)$	-7.44	3.10	1.27
$f_0^{D \rightarrow K_1(1270)}(q^2)$	-1.52	1.10	1.37	$f_0^{D \rightarrow K_1(1400)}(q^2)$	2.70	-1.78	1.37
$f_1^{D \rightarrow K_1(1270)}(q^2)$	0.27	-0.08	1.29	$f_1^{D \rightarrow K_1(1400)}(q^2)$	-0.75	0.26	1.29
$f_2^{D \rightarrow K_1(1270)}(q^2)$	1.68	-0.22	1.31	$f_2^{D \rightarrow K_1(1400)}(q^2)$	-4.00	0.51	1.31
$f_V^{D_s^+ \rightarrow K_1^0(1270)}(q^2)$	1.29	0.93	1.30	$f_V^{D_s^+ \rightarrow K_1^0(1400)}(q^2)$	-9.18	3.91	1.30
$f_0^{D_s^+ \rightarrow K_1^0(1270)}(q^2)$	-2.14	1.49	1.53	$f_0^{D_s^+ \rightarrow K_1^0(1400)}(q^2)$	4.03	-2.59	1.53
$f_1^{D_s^+ \rightarrow K_1^0(1270)}(q^2)$	-0.45	0.14	1.32	$f_1^{D_s^+ \rightarrow K_1^0(1400)}(q^2)$	0.79	-0.06	1.32
$f_2^{D_s^+ \rightarrow K_1^0(1270)}(q^2)$	4.78	-1.42	1.37	$f_2^{D_s^+ \rightarrow K_1^0(1400)}(q^2)$	-7.57	-0.40	1.37

Table 4: Parameters appearing in the fit function for the form factors of the  $D_q \rightarrow K_1(1270)\ell\nu$  and  $D_q \rightarrow K_1(1400)\ell\nu$  decays at  $M_1^2 = 8 \text{ GeV}^2$ ,  $M_2^2 = 6 \text{ GeV}^2$  and  $\theta_{K_1} = 58^\circ$ .

	$a$	$b$	$m_{fit}$		$a$	$b$	$m_{fit}$
$f_V^{D \rightarrow K_1(1270)}(q^2)$	5.48	-1.48	1.23	$f_V^{D \rightarrow K_1(1400)}(q^2)$	2.81	-0.54	1.23
$f_0^{D \rightarrow K_1(1270)}(q^2)$	-2.95	2.02	1.33	$f_0^{D \rightarrow K_1(1400)}(q^2)$	-1.71	1.22	1.33
$f_1^{D \rightarrow K_1(1270)}(q^2)$	0.61	-0.17	1.25	$f_1^{D \rightarrow K_1(1400)}(q^2)$	0.35	-0.12	1.25
$f_2^{D \rightarrow K_1(1270)}(q^2)$	3.90	-0.66	1.29	$f_2^{D \rightarrow K_1(1400)}(q^2)$	2.10	-0.28	1.29
$f_V^{D_s^+ \rightarrow K_1^0(1270)}(q^2)$	7.23	-2.37	1.27	$f_V^{D_s^+ \rightarrow K_1^0(1400)}(q^2)$	2.10	0.66	1.27
$f_0^{D_s^+ \rightarrow K_1^0(1270)}(q^2)$	-4.27	2.83	1.48	$f_0^{D_s^+ \rightarrow K_1^0(1400)}(q^2)$	-2.43	1.67	1.48
$f_1^{D_s^+ \rightarrow K_1^0(1270)}(q^2)$	-0.80	0.14	1.30	$f_1^{D_s^+ \rightarrow K_1^0(1400)}(q^2)$	-0.54	0.15	1.30
$f_2^{D_s^+ \rightarrow K_1^0(1270)}(q^2)$	7.05	0.28	1.36	$f_2^{D_s^+ \rightarrow K_1^0(1400)}(q^2)$	5.62	-1.44	1.36

Table 5: Parameters appearing in the fit function for the form factors of the  $D_q \rightarrow K_1(1270)\ell\nu$  and  $D_q \rightarrow K_1(1400)\ell\nu$  decays at  $M_1^2 = 8 \text{ GeV}^2$ ,  $M_2^2 = 6 \text{ GeV}^2$  and  $\theta_{K_1} = -37^\circ$ .

At the end of this section, we would like to discuss the numeric values of the differential decay rates as well as the branching ratios for the considered semileptonic and nonleptonic transitions.

## semileptonic

The dependence of the longitudinal and transverse components of the differential decay width for the semileptonic  $D_q \rightarrow K_1\ell\nu$  decays is shown in Figs. 9-20 at  $\theta_{K_1} = \pm 37^\circ$ . In these figures, the total decay widths related to each decay are also depicted. To calculate the branching ratios of the semileptonic decays, we Integrate Eq. (30) over  $q^2$  in the whole physical region and using the total mean life-time  $\tau_{D^0} = 0.41 \text{ ps}$ ,  $\tau_{D^+} = 1.04 \text{ ps}$  and  $\tau_{D_s} = 0.50 \text{ ps}$  [23]. The values for the branching ratio of these decays are obtained as presented in Table 7. The errors in this Table are estimated by the variation of the Borel parameters  $M_1^2$  and  $M_2^2$ , the variation of the continuum thresholds  $s_0$  and  $s'_0$  and uncertainties in the values of the other input parameters.

## nonleptonic

For estimating the branching ratio of the nonleptonic  $D \rightarrow K_1\pi$  decay, first the values of the form factors at  $q^2 = m_\pi^2$  are calculated as shown in Table 8. Inserting these values in Eq. (36) and using  $V_{ud} = 0.97377 \pm 0.00027$  [23],  $m_\pi = 0.139 \text{ GeV}$  and  $f_\pi = 0.133 \text{ GeV}$ , we obtain the values for the branching ratio of these decays as presented in Table 9. In comparison, we also include the experimental values and upper limits in this Table. This



	$a$	$b$	$m_{fit}$		$a$	$b$	$m_{fit}$
$f_V^{D \rightarrow K_1(1270)}(q^2)$	3.86	-0.91	1.24	$f_V^{D \rightarrow K_1(1400)}(q^2)$	4.88	-1.28	1.24
$f_0^{D \rightarrow K_1(1270)}(q^2)$	-2.17	1.49	1.35	$f_0^{D \rightarrow K_1(1400)}(q^2)$	-2.57	1.80	1.35
$f_1^{D \rightarrow K_1(1270)}(q^2)$	0.44	-0.10	1.26	$f_1^{D \rightarrow K_1(1400)}(q^2)$	0.56	-0.18	1.26
$f_2^{D \rightarrow K_1(1270)}(q^2)$	2.97	-0.61	1.27	$f_2^{D \rightarrow K_1(1400)}(q^2)$	3.38	-0.48	1.27
$f_V^{D_s^+ \rightarrow K_1^0(1270)}(q^2)$	5.73	-2.15	1.29	$f_V^{D_s^+ \rightarrow K_1^0(1400)}(q^2)$	4.88	-0.48	1.29
$f_0^{D_s^+ \rightarrow K_1^0(1270)}(q^2)$	-3.14	2.07	1.49	$f_0^{D_s^+ \rightarrow K_1^0(1400)}(q^2)$	-3.70	2.50	1.49
$f_1^{D_s^+ \rightarrow K_1^0(1270)}(q^2)$	-0.58	0.08	1.32	$f_1^{D_s^+ \rightarrow K_1^0(1400)}(q^2)$	-0.78	0.17	1.32
$f_2^{D_s^+ \rightarrow K_1^0(1270)}(q^2)$	4.69	0.71	1.35	$f_2^{D_s^+ \rightarrow K_1^0(1400)}(q^2)$	7.84	-1.20	1.35

Table 6: Parameters appearing in the fit function for the form factors of the  $D_q \rightarrow K_1(1270)\ell\nu$  and  $D_q \rightarrow K_1(1400)\ell\nu$  decays at  $M_1^2 = 8 \text{ GeV}^2$ ,  $M_2^2 = 6 \text{ GeV}^2$  and  $\theta_{K_1} = -58^\circ$ .

Table shows that for the  $D^0 \rightarrow K_1^-(1270)\pi^+$ ,  $D^0 \rightarrow K_1^-(1400)\pi^+$  and  $D^+ \rightarrow K_1^0(1400)\pi^+$  cases, the different values of mixing angle  $\theta_{K_1}$  give the values of branching ratios in good agreement with the experimental results but for  $D^+ \rightarrow K_1^0(1270)\pi^+$  decay, the values of the branching ratios at different values of  $\theta_{K_1}$  are about one order of magnitude more than that of the experimental expectation.

In summary, we analyzed the semileptonic  $D_q \rightarrow K_1\ell\nu$  transition with  $q = u, d, s$  in the framework of the three-point QCD sum rules and the nonleptonic  $D \rightarrow K_1\pi$  decay within the factorization approach. We calculated  $D_q$  to  $K_1(1270)$  and  $K_1(1400)$  transition form factors by separating the mixture of the  $K_1(1270)$  and  $K_1(1400)$  states. Using the transition form factors of the  $D \rightarrow K_1$ , we analyzed the nonleptonic  $D \rightarrow K_1\pi$  decay. We also evaluated the decay amplitude and decay width of these decays in terms of the transition form factors. The branching ratios of these decays were also calculated at different values of the mixing angle  $\theta_{K_1}$ . For the non leptonic case, a comparison of the results for the branching ratios with the existing experimental results was also made.

## Acknowledgments

Partial support of Shiraz university research council is appreciated. K. A. would like to thank T. M. Aliev and A. Ozpineci for their useful discussions and also TUBITAK, Turkish Scientific and Research Council, for their partial financial support.

$\theta_{K_1}^\circ$	37	58	-37	-58	
$Br(D^0 \rightarrow K_1^-(1270)\ell\nu)$	$[3.59 \pm 0.29$	$1.03 \pm 0.10$	$5.34 \pm 0.21$	$2.84 \pm 0.25]$	$\times 10^{-3}$
$Br(D^+ \rightarrow K_1^0(1270)\ell\nu)$	$[9.47 \pm 0.45$	$2.70 \pm 0.25$	$14.07 \pm 1.22$	$7.57 \pm 0.35]$	$\times 10^{-3}$
$Br(D_s^+ \rightarrow K_1^0(1270)\ell\nu)$	$[7.84 \pm 0.41$	$2.09 \pm 0.24$	$12.51 \pm 1.16$	$6.91 \pm 0.32]$	$\times 10^{-4}$
$Br(D^0 \rightarrow K_1^-(1400)\ell\nu)$	$[1.09 \pm 0.10$	$1.78 \pm 0.15$	$0.85 \pm 0.02$	$1.20 \pm 0.11]$	$\times 10^{-3}$
$Br(D^+ \rightarrow K_1^0(1400)\ell\nu)$	$[2.93 \pm 0.25$	$4.75 \pm 0.29$	$1.27 \pm 0.10$	$3.20 \pm 0.27]$	$\times 10^{-3}$
$Br(D_s^+ \rightarrow K_1^0(1400)\ell\nu)$	$[3.44 \pm 0.29$	$5.88 \pm 0.34$	$1.49 \pm 0.13$	$3.96 \pm 0.29]$	$\times 10^{-4}$

Table 7: The values for the branching ratio of the semileptonic  $D_q \rightarrow K_1(1270)\ell\nu$  and  $D_q \rightarrow K_1(1400)\ell\nu$  decays at different values of the  $\theta_{K_1}$ .

$\theta_{K_1}^\circ$	37	58	-37	-58	$\theta_{K_1}^\circ$	37	58	-37	-58
$f_V^{D \rightarrow K_1(1270)}$	3.24	1.82	4.04	2.95	$f_V^{D \rightarrow K_1(1400)}$	-3.45	-4.42	2.30	3.65
$f_0^{D \rightarrow K_1(1270)}$	-0.73	-0.42	-0.91	-0.67	$f_0^{D \rightarrow K_1(1400)}$	0.70	0.92	-0.47	-0.75
$f_1^{D \rightarrow K_1(1270)}$	0.34	0.20	0.45	0.32	$f_1^{D \rightarrow K_1(1400)}$	-0.36	-0.49	0.25	0.41
$f_2^{D \rightarrow K_1(1270)}$	2.67	1.55	3.32	2.49	$f_2^{D \rightarrow K_1(1400)}$	-2.81	-3.65	1.87	3.03

Table 8: The values of the form factors of the  $D \rightarrow K_1(1270)$  and  $D \rightarrow K_1(1400)$  for  $M_1^2 = 8 \text{ GeV}^2$ ,  $M_2^2 = 6 \text{ GeV}^2$  at  $q^2 = m_\pi^2$  and different values of the mixing angle  $\theta_{K_1}$ .

$\theta_{K_1}^\circ$	37	58	-37	-58	Exp [23]
$Br(D^0 \rightarrow K_1^-(1270)\pi^+) \times 10^{-2}$	$1.45 \pm 0.11$	$0.75 \pm 0.06$	$2.26 \pm 0.18$	$1.23 \pm 0.11$	$1.15 \pm 0.32$
$Br(D^+ \rightarrow K_1^0(1270)\pi^+) \times 10^{-2}$	$3.75 \pm 0.29$	$1.23 \pm 0.10$	$5.85 \pm 0.37$	$3.18 \pm 0.25$	$< 0.7$
$Br(D^0 \rightarrow K_1^-(1400)\pi^+) \times 10^{-2}$	$0.60 \pm 0.04$	$1.00 \pm 0.12$	$0.26 \pm 0.02$	$0.73 \pm 0.04$	$< 1.2$
$Br(D^+ \rightarrow K_1^0(1400)\pi^+) \times 10^{-2}$	$2.57 \pm 0.21$	$3.63 \pm 0.31$	$1.71 \pm 0.13$	$2.78 \pm 0.24$	$3.8 \pm 1.3$

Table 9: The branching ratios of the nonleptonic  $D \rightarrow K_1(1270)\pi$  and  $D \rightarrow K_1(1400)\pi$  decays at different values of  $\theta_{K_1}$ .

## References

- [1] Ignacio Bediaga, Marina Nielsen, Phys. Rev. D 63, 036001 (2003); arXiv:0304193v1 [hep-ph].
- [2] J. P. Lee, Phys. Rev. D 74, 074001 (2006); H. Hatanaka, K. -C. Yang, Phys. Rev. D 77, 094023 (2008); K. -C. Yang, Phys. Rev. D 78, 034018 (2008).
- [3] M. Suzuki, Phys. Rev. D 47, 1252 (1993).
- [4] M. Bayar, K. Azizi, arXiv:0811.2692 [hep-ph].
- [5] H. Y. Cheng, C. K. Chua, Phys. Rev. D 69, 094007 (2004).
- [6] L. Burakovsky, J. T. Goldman, Phys. Rev. D 57, 2879 (1998); arXiv:9703271 [hep-ph].
- [7] H. Y. Cheng, Phys. Rev. D 67, 094007 (2003).
- [8] T. M. Aliev, V. L. Eletsky, and Ya. I. Kogan, Sov. J. Nucl. Phys. 40, 527 (1984).
- [9] P. Ball, V. M. Braun, and H. G. Dosch, Phys. Rev. D 44, 3567 (1991).
- [10] P. Ball, Phys. Rev. D 48, 3190 (1993).
- [11] A. A. Ovchinnikov and V. A. Slobodenyuk, Z. Phys. C 44, 433 (1989); V. N. Baier and A. Grozin, Z. Phys. C 47, 669 (1990).
- [12] Dong-Sheng Du, Jing-Wu Li and Mao-Zhi Yang, Eur. Phys. J. C 37: 137-184 (2004).
- [13] Mao-Zhi Yang, Phys. Rev. D 73, 034027 (2006); Erratum-ibid. D 73, 079901 (2006).
- [14] P. Colangelo and A. Khodjamirian, in At the Frontier of Particle Physics/Handbook of QCD, edited by M. Shifman (World Scientific, Singapore, 2001), Vol. 3, p. 1495.
- [15] M. Beneke, G. Buchalla, M. Neubert, C. T. Sachrajda, Phys. Rev. Lett. 83, 1914 (1999).
- [16] M. Beneke, G. Buchalla, M. Neubert, C. T. Sachrajda, Nucl. Phys. B 591, 313 (2000).
- [17] M. Beneke, G. Buchalla, M. Neubert, C. T. Sachrajda, Nucl. Phys. B 606, 245 (2001).
- [18] T. M. Aliev, M. Savci, Eur. Phys. J. C 47 (2006) 413.
- [19] K. Azizi, R. Khosravi, F. Falahati, arXiv:0811.2671 [hep-ph].
- [20] G. Buchalla, A. Buras and M. Lautenbacher, Rev. Mod. Phys. 68, 1125 (1996); A. Buras, M. Jamin and M. Lautenbacher, Nucl. Phys. B 400, 75 (1993); M. Ciuchini et al., Nucl. Phys. B 415, 403 (1994); N. Deshpande and X.-G. He, Phys. Lett. B 336, 471 (1994).
- [21] P. Colangelo and F. de Fazio, Phys. Lett. B 520, 78 (2001).

- [22] B. L. Ioffe, *Prog. Part. Nucl. Phys.* 56, 232 (2006).
- [23] C. Amsler et al., Particle Data Group, *Phys. Lett. B* 667, 1 (2008).
- [24] M. Artuso et al., CLEO Collaboration, *Phys. Rev. Lett.* 95, 251801 (2005).
- [25] M. Artuso et al., CLEO Collaboration, *Phys. Rev. Lett.* 99, 071802 (2007).
- [26] P. Ball, R. Zwicky, *Phys. Rev. D* 71, 014015 (2005).
- [27] C. Bourrely, L. Lellouch, I. Caprini, arXiv:0807.2722 [hep-ph].
- [28] D. Becirevic, A. B. Kaidalov, *Phys. Lett. B* 478, 417 (2000).
- [29] V. M. Belyaev, V. M. Braun, A. Khodjamirian, R. Ruckl, *Phys. Rev. D* 51, 6177 (1995).

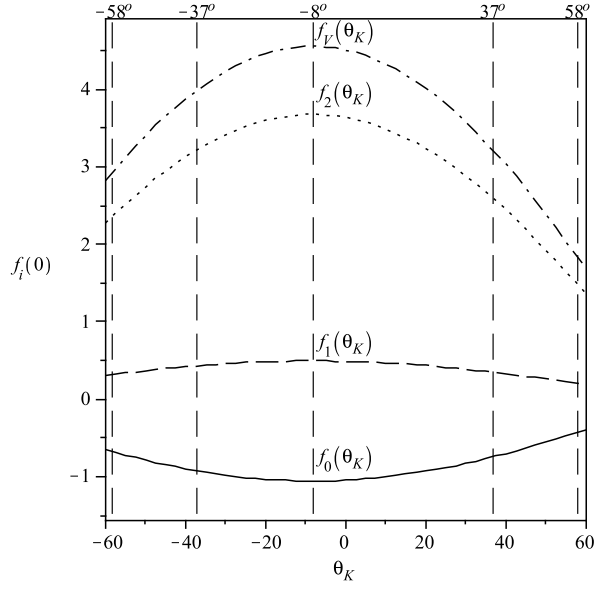


Figure 5: The dependence of the form factors on  $\theta_{K_1}$  at  $q^2 = 0$  for  $D \rightarrow K_1(1270)\ell\nu$  decay.

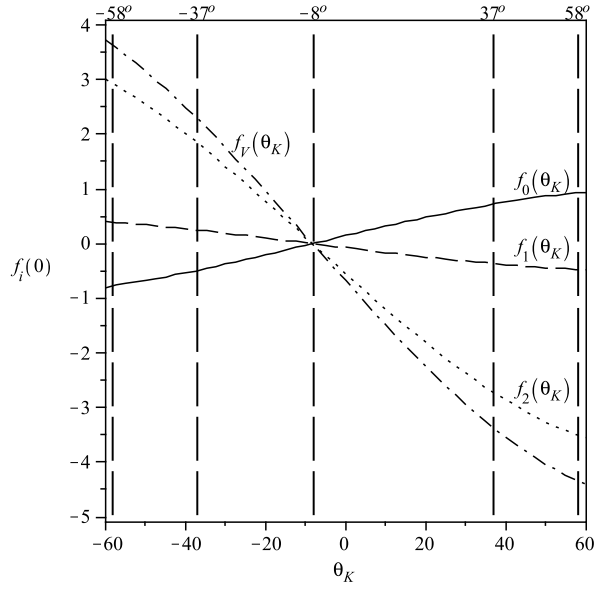


Figure 6: The dependence of the form factors on  $\theta_{K_1}$  at  $q^2 = 0$  for  $D \rightarrow K_1(1400)\ell\nu$  decay.

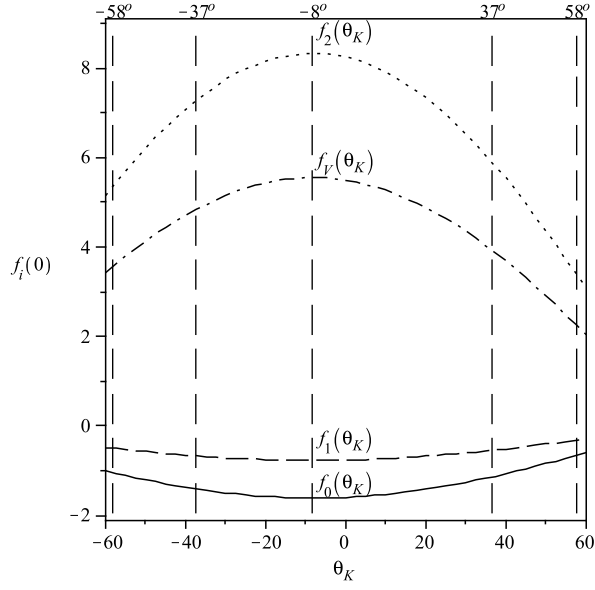


Figure 7: The dependence of the form factors on  $\theta_{K_1}$  at  $q^2 = 0$  for  $D_s \rightarrow K_1(1270)\ell\nu$  decay.

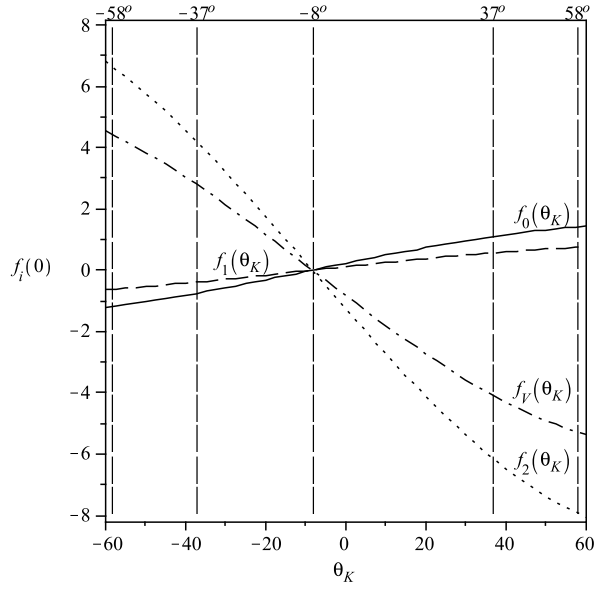


Figure 8: The dependence of the form factors on  $\theta_{K_1}$  at  $q^2 = 0$  for  $D_s \rightarrow K_1(1400)\ell\nu$  decay.

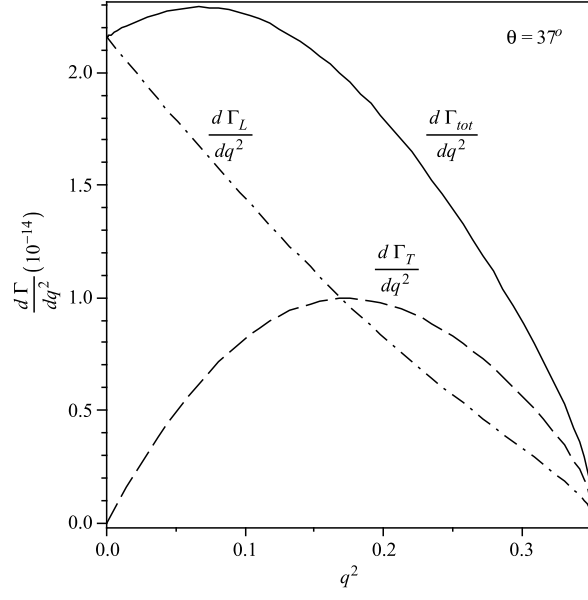


Figure 9: The dependence of the  $d\Gamma_{tot}/dq^2$ ,  $d\Gamma_T/dq^2$  and  $d\Gamma_L/dq^2$  on  $q^2$  at  $\theta_{K_1} = 37^\circ$  for  $D^0 \rightarrow K_1^-(1270)\ell\nu$ .

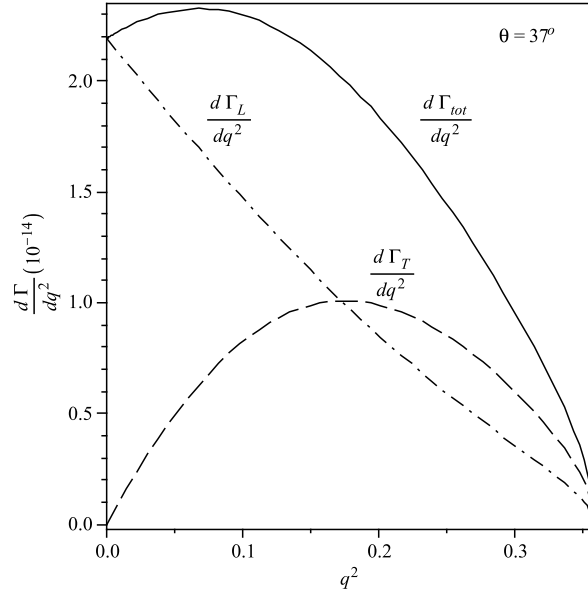


Figure 10: The dependence of the  $d\Gamma_{tot}/dq^2$ ,  $d\Gamma_T/dq^2$  and  $d\Gamma_L/dq^2$  on  $q^2$  at  $\theta_{K_1} = 37^\circ$  for  $D^+ \rightarrow K_1^0(1270)\ell\nu$ .

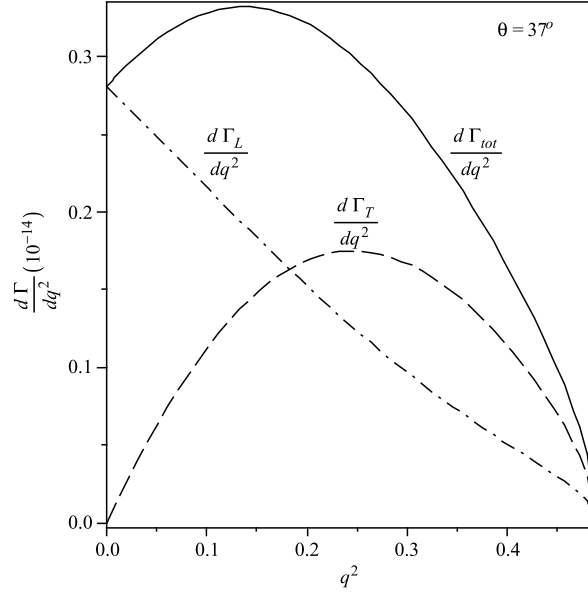


Figure 11: The dependence of the  $d\Gamma_{tot}/dq^2$ ,  $d\Gamma_T/dq^2$  and  $d\Gamma_L/dq^2$  on  $q^2$  at  $\theta_{K_1} = 37^\circ$  for  $D_s^+ \rightarrow K_1^0(1270)l\nu$ .

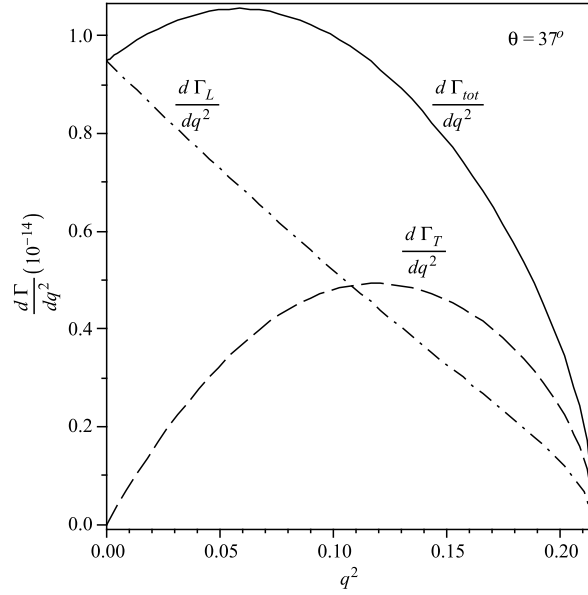


Figure 12: The dependence of the  $d\Gamma_{tot}/dq^2$ ,  $d\Gamma_T/dq^2$  and  $d\Gamma_L/dq^2$  on  $q^2$  at  $\theta_{K_1} = 37^\circ$  for  $D^0 \rightarrow K_1^-(1400)l\nu$ .





Figure 13: The dependence of the  $d\Gamma_{tot}/dq^2$ ,  $d\Gamma_T/dq^2$  and  $d\Gamma_L/dq^2$  on  $q^2$  at  $\theta_{K_1} = 37^\circ$  for  $D^+ \rightarrow K_1^0(1400)l\nu$ .

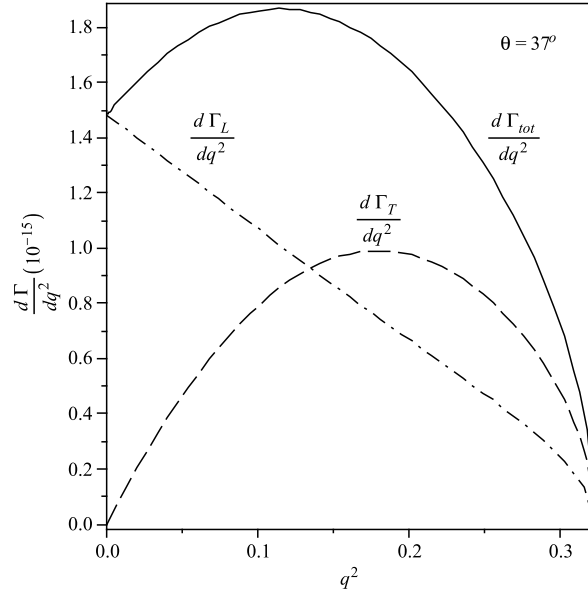


Figure 14: The dependence of the  $d\Gamma_{tot}/dq^2$ ,  $d\Gamma_T/dq^2$  and  $d\Gamma_L/dq^2$  on  $q^2$  at  $\theta_{K_1} = 37^\circ$  for  $D_s^+ \rightarrow K_1^0(1400)l\nu$ .

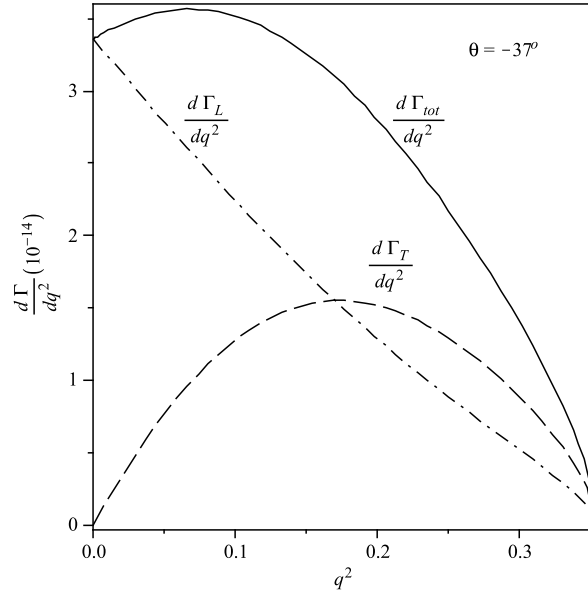


Figure 15: The dependence of the  $d\Gamma_{tot}/dq^2$ ,  $d\Gamma_T/dq^2$  and  $d\Gamma_L/dq^2$  on  $q^2$  at  $\theta_{K_1} = -37^\circ$  for  $D^0 \rightarrow K_1^-(1270)\ell\nu$ .

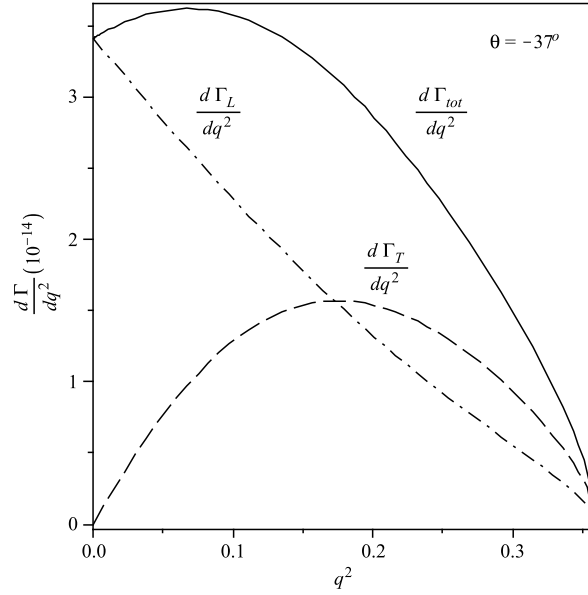


Figure 16: The dependence of the  $d\Gamma_{tot}/dq^2$ ,  $d\Gamma_T/dq^2$  and  $d\Gamma_L/dq^2$  on  $q^2$  at  $\theta_{K_1} = -37^\circ$  for  $D^+ \rightarrow K_1^0(1270)\ell\nu$ .

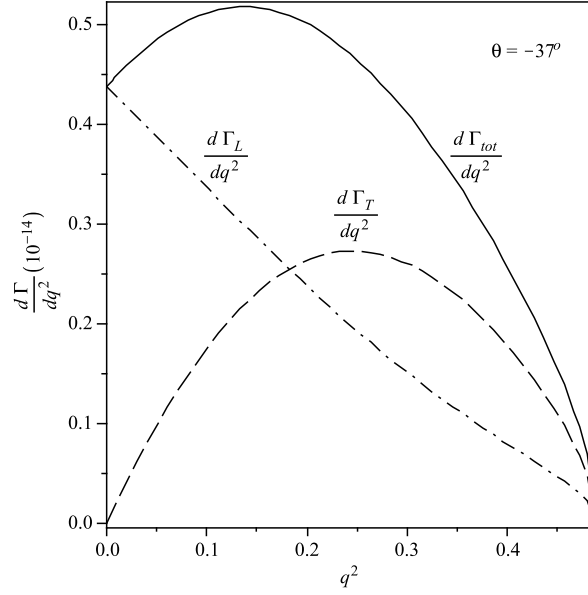


Figure 17: The dependence of the  $d\Gamma_{tot}/dq^2$ ,  $d\Gamma_T/dq^2$  and  $d\Gamma_L/dq^2$  on  $q^2$  at  $\theta_{K_1} = -37^\circ$  for  $D_s^+ \rightarrow K_1^0(1270)\ell\nu$ .

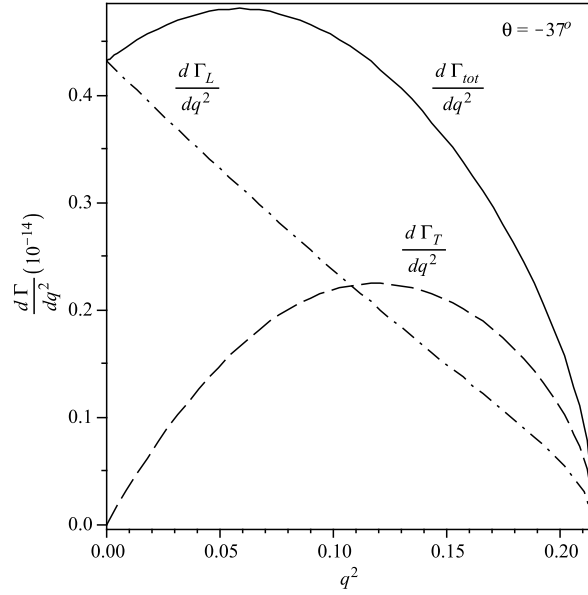


Figure 18: The dependence of the  $d\Gamma_{tot}/dq^2$ ,  $d\Gamma_T/dq^2$  and  $d\Gamma_L/dq^2$  on  $q^2$  at  $\theta_{K_1} = -37^\circ$  for  $D^0 \rightarrow K_1^-(1400)\ell\nu$ .

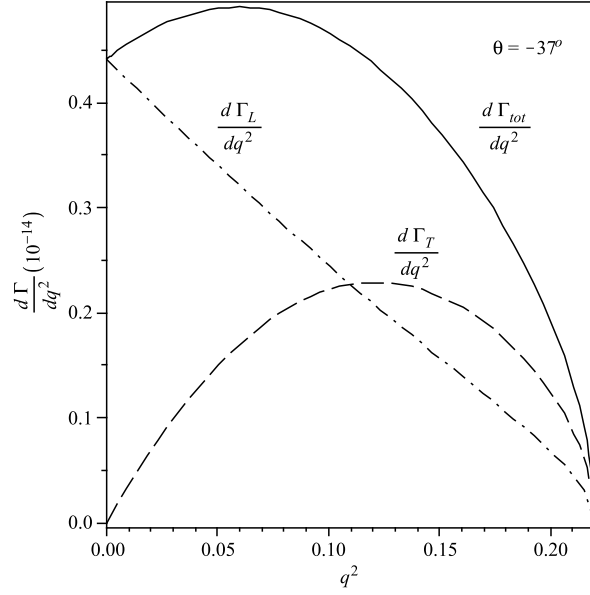


Figure 19: The dependence of the  $d\Gamma_{tot}/dq^2$ ,  $d\Gamma_T/dq^2$  and  $d\Gamma_L/dq^2$  on  $q^2$  at  $\theta_{K_1} = -37^\circ$  for  $D^+ \rightarrow K_1^0(1400)\ell\nu$ .

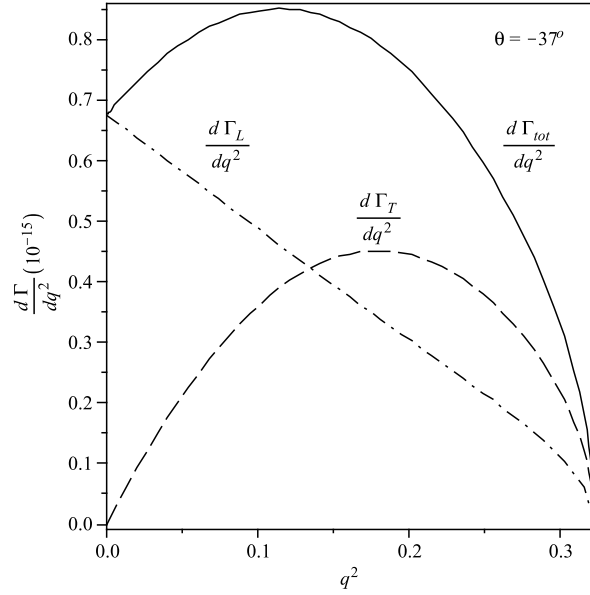


Figure 20: The dependence of the  $d\Gamma_{tot}/dq^2$ ,  $d\Gamma_T/dq^2$  and  $d\Gamma_L/dq^2$  on  $q^2$  at  $\theta_{K_1} = -37^\circ$  for  $D_s^+ \rightarrow K_1^0(1400)\ell\nu$ .